

ENVIRONMENTAL INFLUENCES ON VERTICAL PICOPLANKTON
DISTRIBUTION IN MĀMALA BAY, O‘AHU, HAWAI‘I

A THESIS SUBMITTED TO
THE GLOBAL ENVIRONMENTAL SCIENCE
UNDERGRADUATE DIVISION IN PARTIAL FULFILLMENT
OF THE REQUIREMENTS FOR THE DEGREE OF

BACHELOR OF SCIENCE

IN

GLOBAL ENVIRONMENTAL SCIENCE

MAY 2021

By
MARIAM G. MORENO

Thesis Advisors

MARGARET A. MCMANUS
CHRISTINA M. COMFORT

We certify that we have read this thesis and that, in our opinion, it is satisfactory in scope and quality as a thesis for the degree of Bachelor of Science in Global Environmental Science.

THESIS ADVISORS

Professor Margaret A. McManus
Department of Oceanography

Christina M. Comfort
Department of Oceanography

For my Tia Coca who was my motivation and support throughout my college career. I love and miss you so much.

ACKNOWLEDGEMENTS

I want to extend my utmost gratitude to Dr. Margaret McManus for granting me this wonderful opportunity in her lab. Dr. Jeffrey Drazen, for advising me every step of the way. Christina Comfort for mentoring me in this thesis project and teaching me so much in the lab. I want to thank my family and my friends for supporting me throughout my college career. And lastly, I want to thank all the faculty and staff of SOEST for guiding and educating me in my academia.

ABSTRACT

Picoplankton are phytoplankton between 0.2 and 2.0 μm in diameter that contribute significantly to marine primary productivity. We investigated the distributions of two genera of picoplankton, *Prochlorococcus* and *Synechococcus*, in the nearshore environment of Māmalā Bay, O‘ahu. The focus of this study is to analyze the influences on the vertical distribution of the two populations. Picoplankton samples from each site were counted with a flow cytometer, these counts were compared to environmental factors: nutrients, chlorophyll, and Photosynthetically Active Radiation (PAR). Both *Prochlorococcus* and *Synechococcus* distributions are influenced by all these factors, especially nutrients and mixing events. Both populations follow a specific pattern that is unique to nearshore ecosystems in the subtropical North Pacific Ocean dictated by the underlying nutricline and seasonal variability in Māmalā Bay.

TABLE OF CONTENTS

Dedication	iii
Acknowledgements	iv
Abstract	v
List of Tables	vii
List of Figures	viii
1.0 Introduction	9
1.1 Phytoplankton Ecology in the Pelagic	9
1.2 Seasonal Trends	11
1.3 Nearshore Ecology: Māmala Bay	13
2.0 Methods	15
2.1 Study Site	15
2.2 Field Procedure	17
2.3 Flow Cytometry	17
2.4 Nutrient and Chlorophyll Analysis	18
2.5 Station ALOHA	18
2.6 Data Visualization and Analysis	19
3.0 Results	20
3.1 Environmental Properties of Māmala Bay	20
3.2 Cell Abundances	26
3.2.1 Vertical Patterns of <i>Prochlorococcus</i> and <i>Synechococcus</i> Distributions	26
3.2.2 Comparisons Between Māmala Bay Stations	26
3.3 Comparisons with Oceanographic Measurements	28
3.3.1 Māmala Bay Comparisons	28
3.3.2 Station ALOHA Comparisons	32
3.4 Seasonal Variations	33
4.0 Discussion	40
4.1 Seasonality	40
4.2 Nearshore Distribution of <i>Prochlorococcus</i> and <i>Synechococcus</i>	42
4.3 Ecosystem Services	43
5.0 Conclusion	45
Literature cited	46

LIST OF TABLES

Table 1. PAR values	23
Table 2. Depth of Environmental Parameters for Station 1.....	34
Table 3. Depth of Environmental Parameters for Station 2.....	35
Table 4. Depth of Environmental Parameters for Station 3.....	36

LIST OF FIGURES

Figure 1. Maps of Sample Sites	16
Figure 2. Temperature Plots for each Station	21
Figure 3. Average Chlorophyll-a Distribution for each Station	24
Figure 4. Deep Chlorophyll Maximum Depths of each Cruise	24
Figure 5. Average Nutrient Distribution for each Station.....	25
Figure 6. Average Cell Abundances for each Station.....	27
Figure 7. Chlorophyll and Cell Correlations of each Station.....	28
Figure 8. Nutrient and Cell Correlations of each Station	29
Figure 9. PAR and Cell Correlations of each Station.....	30
Figure 10. PAR Comparisons for Māmalala Bay.....	31
Figure 11. Chlorophyll and Cell Correlations for Station ALOHA.....	32
Figure 12. Nutrient and Cell Correlations for Station ALOHA.....	33
Figure 13. Seasonal Profiles of <i>Prochlorococcus</i> and <i>Synechococcus</i>	37

1.0 INTRODUCTION

1.1 Phytoplankton Ecology

Photosynthetic phytoplankton measuring in length between 0.2 and 2.0 μm in diameter are referred to as picoplankton. They are responsible for over 90% of primary productivity in the ocean (Karl and Letelier, 2008). The two genera of picoplankton of interest in this study are *Prochlorococcus* and *Synechococcus*. *Prochlorococcus* is smaller in size (0.6 μm) and is more abundant in oligotrophic water. *Synechococcus* is larger in size (0.9 μm) (Morel et al. 1993) and is more abundant in regions where nutrients are more abundant at the surface (Campbell et al., 1997). Picoplankton distribution is reflected in the chlorophyll concentrations that is influenced by photosynthetically active radiation (PAR) and nutrients. PAR is the available solar energy for photosynthesis, which decreases with depth starting at the surface (Frouin & Murakami, 2007). Picoplankton are most abundant in the region of the euphotic zone with the highest availability of PAR (Malmstorm et al. 2010). The distribution of chlorophyll-a in the water column reflects phytoplankton biomass, which is influenced by light availability and nutrients (Huisman et al., 2006). In general, chlorophyll concentrations increase with depth until they reach a subsurface maximum at the deep chlorophyll maximum (DCM) and then decrease to the bottom of the euphotic zone (Cullen, John J., 1982). The depth of the DCM in oligotrophic regions will be deeper compared to areas of upwelling (Wang et al. 2009). Nutrients brought to the surface by upwelling support enhanced primary productivity at shallower depths compared to surface waters that are depleted of nutrients.

The population dynamics of both *Prochlorococcus* and *Synechococcus* are related to a variety of processes including nutrient recycling and mixing. The nutricline is defined where nitrite and nitrate increase to 0.1 μM (Campbell et al. 1997). The nutrient supply in oligotrophic waters is controlled by upwelling and mixing (Karl & Letelier 2008). Picoplankton use available light and nutrients for primary productivity. Turbulence at the surface from wind and waves, as well as convective overturn from evaporation or air temperature, play a role in homogenizing physical properties at a range of near surface depths creating the mixed layer. The mixed layer depth (MLD) is characterized by a nearly uniform temperature and salinity distribution (Kato & Phillips, 1969). All these factors contribute to the vertical distribution of picoplankton in the subtropics.

Station ALOHA is a 6-mile radius research site located within the North Pacific Subtropical Gyre (NPSG). *Prochlorococcus* and *Synechococcus* have been measured at Station ALOHA at magnitudes of 36.8E9 to 336.3E9 cells m^{-3} and 5.4E9 cells m^{-3} (Rii et al. 2016). Both genera of picoplankton are present at the surface and extend to the bottom of the euphotic zone. *Prochlorococcus* is the dominant picoplankton genus and exists as high-light and low-light ecotypes at Station ALOHA (Partensky et al. 1999, Campbell et al. 1997, Malmstorm et al. 2010). Due to light-adaptive properties, *Prochlorococcus* can extend to the bottom of the photic zone (Partensky et al. 1999). *Synechococcus* has only been observed in the upper region of the euphotic zone, which is approximately the first 100 meters. *Synechococcus* has a distinct distribution of primarily occupying the surface waters.

The picoplankton at Station ALOHA rely on nutrients provided by nitrogen fixation that occurs in the surface waters that are well-illuminated. This is because the nutrient profile at Station ALOHA has a low nitrate-to-phosphate ratio in the upper 200 meters (Rii et al. 2016). In the event that nitrate becomes available, it is quickly assimilated for phytoplankton productivity (Karl & Letelier, 2008). Nutrients remain in limited supply since phytoplankton productivity relies on their constant recycling.

The picoplanktonic response to the oligotrophic environment is also evident in their contributions to chlorophyll and carbon biomass. *Prochlorococcus* contributed 34-35% of the carbon biomass in the euphotic zone at Station ALOHA. (Campbell et al. 1997). Picoplankton also contribute over 60% of chlorophyll-a in nitrate-limited conditions (such as Station ALOHA) (Campbell et al. 1997). In the Atlantic, the Bermuda Atlantic Time Series (BATS) showed that *Prochlorococcus* and *Synechococcus* have similar distributions with *Prochlorococcus* abundances peaking in the summer, and *Synechococcus* peaking in the winter (Malmstorm et al. 2010).

1.2 Seasonal Trends

The seasonal cycles of the environmental parameters in the pelagic environment cause a vertical shift in picoplankton abundances over time. Wind, rain, storm events, and climate fluctuations such as El Niño Southern Oscillation (ENSO) can influence changes in seasonal cell abundance maximums as well as the magnitude in the shift of environmental parameters. Generally, the NPSG experiences northeasterly trades, however during an ENSO period those winds are weakened, resulting in more stratified water conditions (Campbell et al. 1997). This tends to cause an upward vertical shift in

the MLD, nitracline, and DCM (Campbell et al., 1997). *Prochlorococcus* measurements show a minimum surface abundance in the winter and a maximum surface abundance in late summer and fall. *Synechococcus* measurements show the reverse pattern at Station ALOHA (Campbell et al., 1997; Malmstorm et al., 2010). Measured *Prochlorococcus* abundances varied two-fold between summer and winter months, and *Synechococcus* abundances varied three or four-fold (Campbell et al. 1997). The seasonal subsurface maximums coincide with periods of shallow MLD and availability of nutrients.

Wind and rain events provide the largest seasonal impacts in the North Pacific Ocean and influence the vertical picoplankton distributions, especially at the surface. Depths of the nutricline, thermocline, and DCM will fluctuate despite little variance in seasons. Campbell et al. (1997) revealed that weakening trade winds associated with ENSO impacted these depths between a 1991-1994 study conducted at Station ALOHA. Campbell et al. (1997) revealed that the nutricline was shallowest in the winter and deepest in the spring. Seasonal cycles of chlorophyll-a concentrations had different patterns in the upper and lower portions of the euphotic zone. During the winter months, chlorophyll-a concentrations increased in the euphotic zone. This was the consequence of a photoadaptive response to low light intensity. The seasonal chlorophyll-a maximum during May to June in the lower euphotic zone was the result of a change in primary productivity and biomass as a result of increased light intensity in summer (Campbell et al. 1997).

The picophytoprokaroytic carbon is one way to quantify cells throughout the mixed layer and at the bottom of the euphotic zone (Yoshimi et al., 2016). Partensky et al. (1999) observed at Station ALOHA that *Prochlorococcus* accounted for

approximately 3/4 of picophytoprokaryotic carbon during summer months, and *Synechococcus* had its highest picophytoprokaryotic carbon count in the winter months when nutrient concentration is higher. *Prochlorococcus* had a more prominent presence during the warmest months of the year when nutrient concentrations were lower. A strong relationship between nutrient availability and primary productivity is evident at Station ALOHA (Yoshimi et al., 2016).

1.3 Nearshore Ecology: Māmala Bay

The vertical distributions of phytoplankton near the island of O‘ahu are likely to have similarities to station ALOHA but may additionally be influenced by the proximity to the island. The relationship between these factors are reflected in the chlorophyll concentrations, which are partially produced by *Prochlorococcus* and *Synechococcus* cells (among other photoautotrophs). *Prochlorococcus* and *Synechococcus* populations are predicted to follow a nearshore distribution laid out by Partensky et al. (1999) that describes an abundance of cell concentrations in the surface mixed layer and a decrease below the thermocline. In Māmala Bay, a subsurface maximum in chlorophyll-a fluorescence and phytoplankton biomass is observed (Huisman et al., 2006). In a nearshore ecosystem, the marine ecosystem is heavily influenced by the land-derived nutrients, changes in circulation patterns and increased turbidity.

The proximity of Māmala Bay to the island of O‘ahu may have an effect on the seasonality cell distribution, especially in the euphotic zone. Via the island mass effect, islands such as O‘ahu may act as a source of nutrients that can fertilize nearshore or offshore nutrient-depleted waters (Messie et al. 2020). Runoff and groundwater

originating from the landmass of the island and potential increased upwelling introduces additional nutrients to near-island waters as compared to open-ocean water. As a result, chlorophyll concentrations increase next to the island (Gove et al. 2016). The increase of these environmental factors leads to the increase of phytoplankton biomass in these ecosystems. The island mass effect in oligotrophic oceanic regions occurs can also occur when phytoplankton get carried away from the island by ocean currents and lead to a bloom in a “delayed” island mass effect (Messie et al. 2020). The localized increase in phytoplankton biomass near the island stimulates processes that enhance nutrient concentration (Gove et al. 2016). This results from increased turbidity that occurs from phytoplankton blooms that hinder the intensity of PAR penetration.

The goal of this study is to compare nearshore vertical picoplankton distributions in an onshore-offshore gradient and to compare these results with pelagic picoplankton distribution patterns at Station ALOHA, which has a long, rich history of observations. The analysis of the influences from environmental factors will allow a better understanding of picoplankton distributions relative to a nearby island. Given past observations on *Prochlorococcus* and *Synechococcus* distributions in pelagic environments in the Northern Pacific Ocean, we hypothesize that nearshore distributions are also influenced heavily by nutrients. Station ALOHA will be used as a reference for comparison of the vertical distribution of both genera of picoplankton. We hypothesize that the offshore sample site will be most similar Station ALOHA. Keeping the nearshore distribution for both populations in mind, we will apply the results of this study to better define the environmental properties and vertical ecology of Māmala Bay to enhance our knowledge of nearshore vertical picoplankton distribution.

2.0 METHODS

2.1 Study Site

Māmala Bay is on the southern shore of the island of O‘ahu, Hawai‘i. All vessels entering the principal seaport of the State of Hawai‘i, Honolulu Harbor, must enter through Māmala Bay. The south shore slope off the coast of O‘ahu is steep with intricate bathymetry associated with coral reefs (Souza and Powell, 2017). Māmala Bay experiences internal waves generated at flanks of ridges at the southeastern corner of O‘ahu (Comfort et. al 2015). Over an 8 year period from 2012-2020, samples for 32 cruises were collected and analyzed to create a time-series of data that displays the physical properties and ecology of Māmala Bay. Data were collected from three sites, Station 1 at 21.279305 °N, 157.872347 °W, Station 2 at 21.276265 °N, 157.873978 °W, and Station 3 21.22333917 °N, 157.8648714 °W. These locations represent two nearshore environments (1.6 km and 2 km from shore) and one offshore environment (7 km from shore). The nearshore sites are labeled S1 and S2, and the offshore site is labeled S3 in Figure 1¹. The island of O‘ahu shields Stations 1 and 2 from east-northeasterly trade winds, while Station 3 is more exposed to the trades (Comfort, et al.

¹ Each sampling station was taken from the former Seawater Air Conditioning (SWAC) project of Downtown Honolulu. The two nearshore sites served as potential warm water discharge sites, and the offshore site served as a potential cold water intake site. More information at <https://hahana.soest.hawaii.edu/cmoreswac/cmoreswac.html>

2015). Typical weather conditions during sampling were calm with a few occurrences of strong winds and currents that occasionally hindered sampling at Station 3.

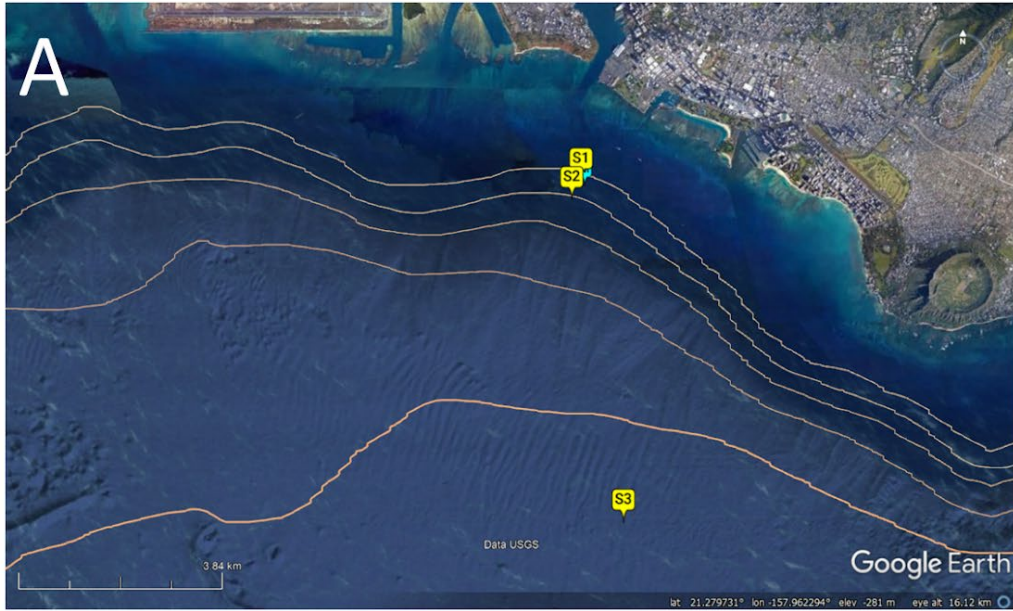


Figure 1. (A) Map of all three sampling sites and mooring with bathymetric contour lines. (B) Map zoomed in on nearshore sites Station 1 and 2 along with the marked mooring site. Bathymetric contours lines indicate depth and steepness of slope.

2.2 Field Procedure

Seawater samples were collected in 12 8-liter Niskin bottles that were attached to a conductivity-temperature-depth (CTD) rosette. The CTD was also equipped with auxiliary sensors that provided additional profiles for dissolved oxygen, chlorophyll fluorescence, turbidity, and PAR. Samples that were taken from the 8-liter Niskin bottles were analyzed for nitrate, chlorophyll-a, and picoplankton cells. Over 32 cruises, Niskin bottles were sampled at Station 1 at 5, 25, 45, 75, and 100 meters, Station 2 at 5, 25, 45, 75, 100, 125, and 150 meters, and Station 3 at 5, 25, 45, 75, 100, 150, 300, and 500 meters. Each picoplankton sample was transferred with a 15 milliliter falcon tube from the niskin bottle into 2 milliliter aliquots. Picoplankton samples were then preserved with 30 microliters of 16% paraformaldehyde (0.24% total concentration) and flash frozen in liquid nitrogen and stored at -80°C until analysis.

2.3 Flow Cytometry

A staff member of the McManus lab counted picoplankton cells with a Cytocopia Influx Flow Cytometer equipped with a black ceramic nozzle tip, 488 and 457 nanometer lasers, and a small-particle forward scatter detector (FSC). The instrument was aligned to minimize noise and optimize resolution of particles. Heineken beer was used to align and focus lasers with the flow stream. The fluorescence of the beer was consistent with 488 and 457 nanometer light. Beer was stored at -20°C in 1 milliliter aliquots and used daily to align instruments. 1 micrometer spherical Ultra-Rainbow beads were used to fine tune the

laser, stream alignment, and align FSC detector. 1 drop of beads was diluted in 2 milliliters of filtered Milli-Q water. Station ALOHA samples from surface water and the DCM were used as quality control to ensure the alignment would discern cell populations from noise and resolve populations. A set of aliquots containing the quality control samples was spiked with 2 microliters of bead dilution. Samples from each site were spiked with 0.2 microliters of bead dilution. 100 microliters of data were collected for each sample, enumerating populations of *Prochlorococcus* and *Synechococcus*. All data were collected in a list format using the Spigot program. The two populations were distinguished according to their fluorescence and forward scatter signals in the FlowJo program.

2.4 Nutrient and Chlorophyll Analysis

Nutrient samples were stored frozen at -20°C until analysis. Each sample was processed with an AA3 nutrient analyzer. The nutricline is determined by the depth at which nitrate concentrations exceeded 0.1 $\mu\text{mol/kg}$ based on a linear interpolation of the bottle sample data. Chlorophyll samples were filtered onto 25 mm GF/F glass fiber filters after each cruise and then were extracted in acetone for at least 5 days. All chlorophyll samples were analyzed with a Turner-10AU fluorometer.

2.5 Station ALOHA

Data from Station ALOHA were downloaded from <https://hahana.soest.hawaii.edu/hot/hot-dogs>. The variables downloaded included *Prochlorococcus* and *Synechococcus* concentrations, nutrient bottle concentrations, and

chlorophyll bottle concentrations. Data from the 2012-2020 time frame were used to overlap with the time period of the Māmala Bay sampling.

2.6 Data Visualization and Analysis

Visualizations of the data and correlations were created in MATLAB. The physical properties from each station were correlated to cell abundances from their corresponding stations to investigate the influences on vertical picoplankton distribution. Data for PAR, nutrients, and cell counts were log-transformed for plotting. To examine seasonality, seasons were defined as: winter (January- March), spring (April-June), summer (July-September) and fall (October-December). Cell counts were averaged during these time periods at each station. The MLD, DCM, and nutricline were calculated for each season at each station. The MLD was determined by the depth at which the density was 0.125 kg/m^3 greater than the surface density.

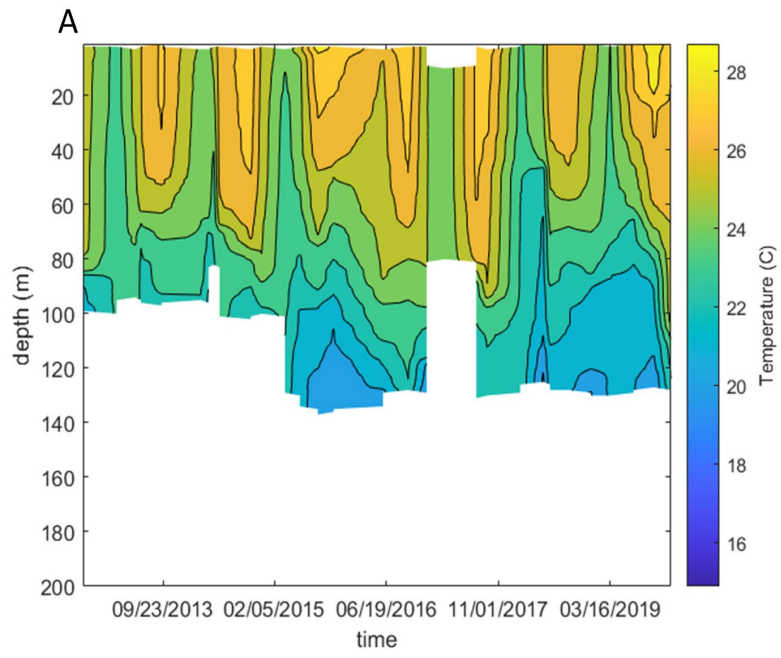
3.0 RESULTS

3.1 Environmental Properties of Māmala Bay

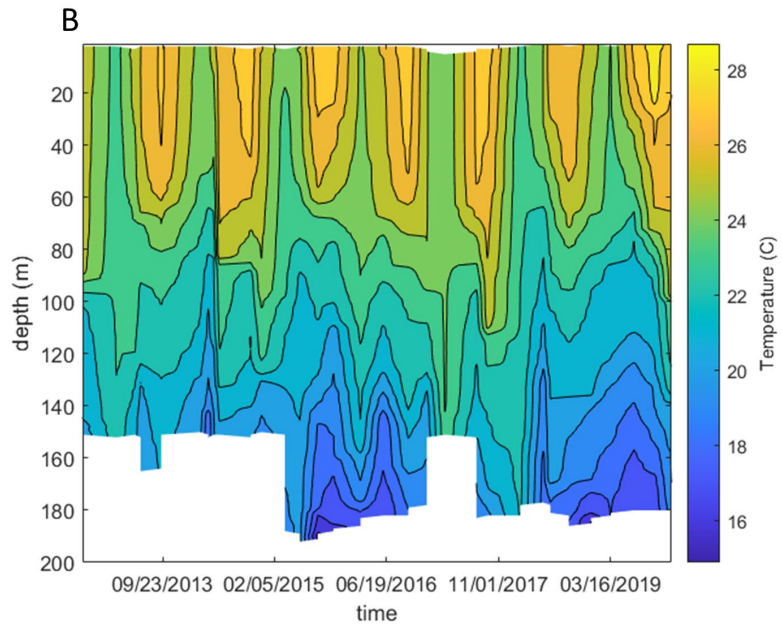
The results from the Māmala Bay sampling stations highlight the ecology and physical structure in the first 200 meters where light intensity can penetrate for primary productivity.

Temperature. Temperature varied by roughly 10°C at each station. Temperature decreases with depth, and the depths of the thermocline vary between seasons (Figure 2). In summer months when air temperatures are higher, the surface warms and the thermocline is located between 60-80 meters in the water column. The thermocline in the winter months is located between 100-120 meters in the water column.

Station 1



Station 2



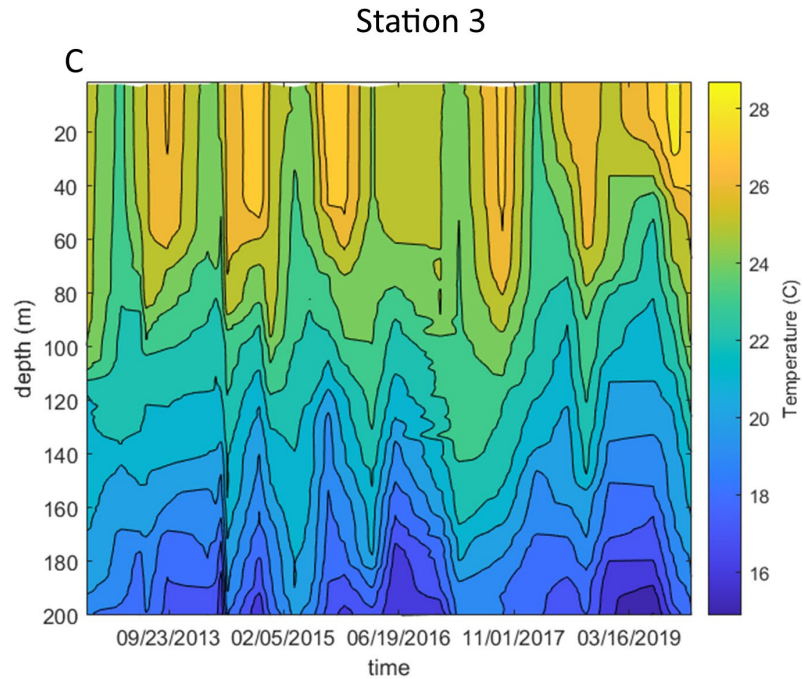


Figure 2. Temperature profile of each cruise from 2012-2020. (A) is the profile for station 1. (B) is the profile for station 2. (C) is the profile for station 3. The color bar shows the range of temperature from 15-28°C. The y axis extends to 200 meters for all plot

PAR. PAR decreased logarithmically with depth. PAR at each bottle sample depth from stations 1, 2, and 3 is given in Table 1. Depths where PAR values reach 1% and 0.1% of the surface value are shown in Table 1. The depths at which surface light levels reached 1% and 0.1% were similar for both nearshore sites. The 1% and 0.1% light levels were deeper at the offshore site than the nearshore sites.

Table 1. Surface PAR values of each station and the depths where those levels are present. The values and depths of where PAR reaches 1% and 0.1% of the surface values are also given. PAR is measured in $\mu\text{E}/\text{m}^2/\text{s}$ and depth is measured in meters.

	Surface PAR ($\mu\text{E}/\text{m}^2/\text{s}$)	Depth (m)	1% ($\mu\text{E}/\text{m}^2/\text{s}$)	Depth (m)	0.1% ($\mu\text{E}/\text{m}^2/\text{s}$)	Depth (m)
Station 1	2452.24	3	23.7	78	2.43	95
Station 2	1914.87	3	19.35	72	1.94	101
Station 3	1717.34	3	16.56	99	1.74	150

Chlorophyll. In Māmala Bay, fluorometric chlorophyll-a concentrations from bottle samples were typically highest at 75 m at stations 1 and 2, and highest at 100 m at station 3. (Figure 3). All stations had shifts in DCM depth according to seasons. Deeper DCM depths were observed in the summer months, and shallower DCM depths were observed in the winter (Figure 4). *In situ* optical fluorescence data revealed average DCM depths for stations 1, 2, and 3 were 66.5 meters, 69.9 meters, and 94.6 meters (Tables 3-5), respectively. Across all stations, the largest decrease in DCM depth occurred between the summer and fall months.

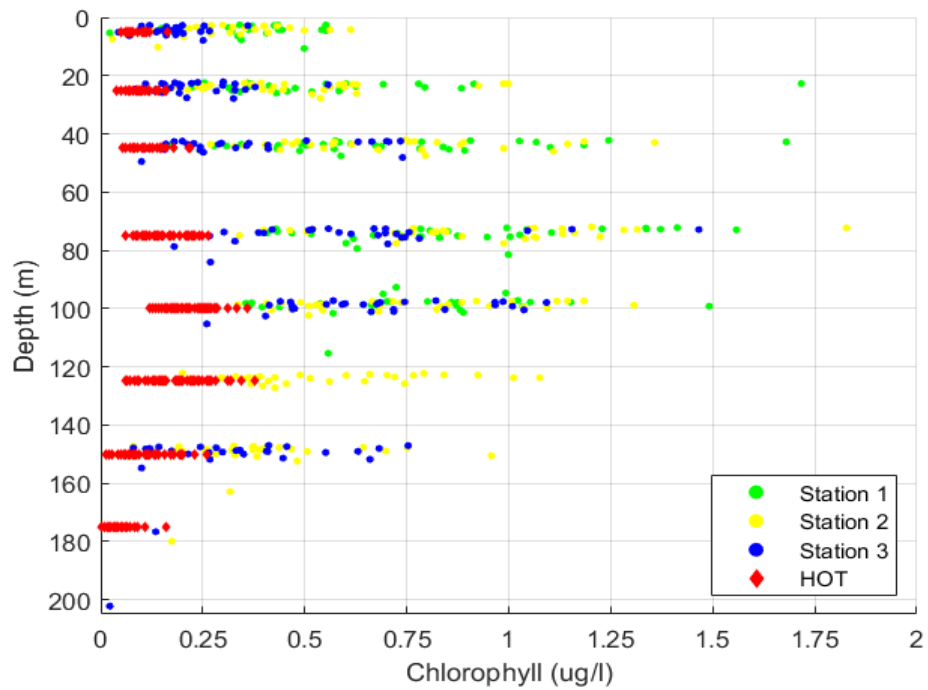


Figure 3. Depth distribution of chlorophyll-a (ug/l) collected from niskin bottles at the sample depths (m) from all three stations. Green dots represent station 1, yellow represents station 2, and blue represents station 3. The red diamonds represent the data from Station ALOHA.

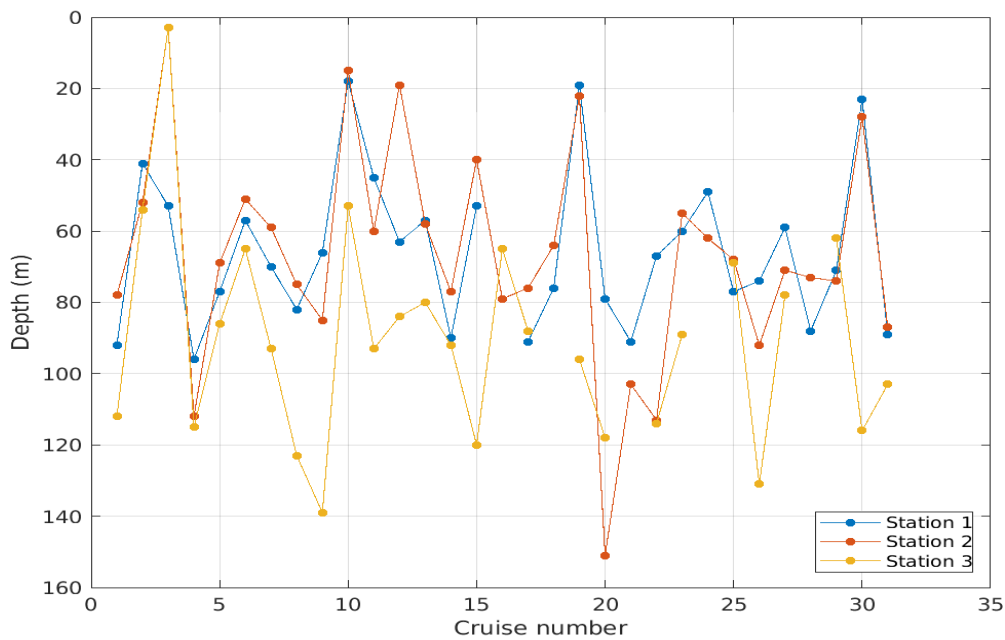


Figure 4. Deep chlorophyll maximum (DCM) for each cruise at each of the three stations. DCM depths were identified based on maximum chl-a reading from the ECO-FLNTU fluorometer. Breaks in the lines indicate time points with no data. Blue lines represent station 1, red lines represent station 2, and orange lines represent station 3.

Nitrate. Nitrate concentrations were $<0.5 \mu\text{mol/kg}$ in the upper euphotic zone. The nutricline depth ranged from about 75 to 100 meters. By 150 meters depth, nitrate concentrations range from $0.5\text{-}3.5 \mu\text{mol/kg}$. Similar distributions were seen across all stations. The nitrate distribution of each station compared to the nitrate distribution of Station ALOHA is shown in Figure 5. The nutricline at Station ALOHA is deeper relative to the nutricline of Māmalala Bay, and the nitrate content was relatively lower compared to the Māmalala Bay stations. Station ALOHA did not show significant increase in nitrate until approximately 100 meters (Figure 5) Nitrate concentrations begin to exceed $0.5 \mu\text{mol/kg}$ at 100 meters and continue to increase until about 175 meters where nitrate reaches nearly $3.5 \mu\text{mol/kg}$.

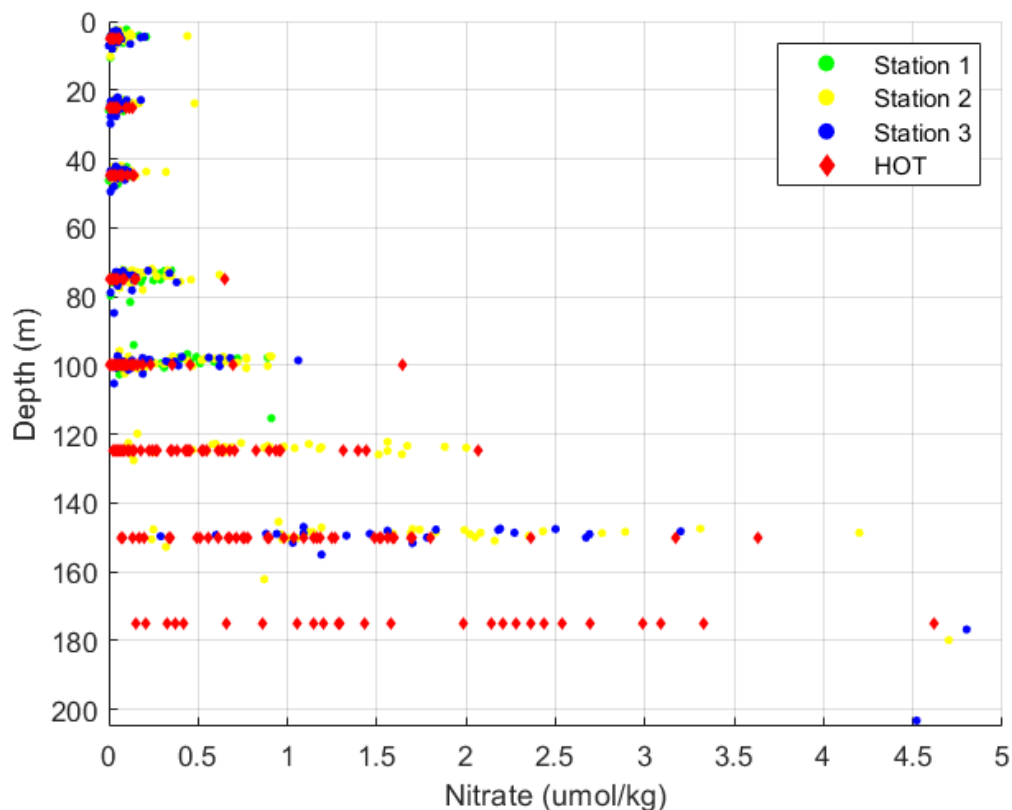


Figure 5. Distribution of nutrients ($\mu\text{mol/kg}$) collected from Niskin bottles at the corresponding depths (m) from all three stations. Green dots represent station 1, yellow represents station 2, and blue represents station 3. The red diamonds represent data from Station ALOHA.

3.2 Vertical Distributions of Cell Abundances

3.2.1 Vertical Patterns of *Prochlorococcus* and *Synechococcus* Distributions

Māmala Bay stations and Station ALOHA shared similar vertical distributions for each of the cell types. At the Māmala Bay stations, *Prochlorococcus* distributions had an increase in cell abundance between 5 and 45 meters. Between 45 to 75 meters, counts decreased drastically and continued decreasing until 150 meters. Counts at the Station ALOHA profile increased until 75 meters, then decreased between 75 and 100 meters (Figure 6). *Synechococcus* distributions continually decreased from the surface to 150 meters at all Māmala Bay stations (Figure 7). There is also a rapid decrease between 45 and 75 meters with *Synechococcus* cells. However, station 3 experiences an increase in cell counts from the surface to 45 meters depth. After this maximum, *Synechococcus* then begins to decrease until 150 meters. The cell abundances at Station ALOHA experience a slight increase from 5 to 75 meters. After 75 meters, cell counts decrease until they nearly disappear by 150 meters.

3.2.2 Comparison between Māmala Bay Stations

Station 3 had the highest abundances of *Prochlorococcus* at each depth compared to stations 1 and 2. The median of cell abundances at station 3 reached about $2.0\text{E}5$ cells/ml at their maximum, and cell counts reduce to about $0.1\text{E}5$ cells/ml at their minimum offshore. Station 2 had higher *Prochlorococcus* abundances until 45 meters,

and then dropped lower than station 1 counts. Cell counts at station 2 reached about $0.1E5$ cells/ml at the bottom of the sample depth of 150 meters. As station 1 only extends 100 meters, cell counts did not drop lower than $0.5E5$ cells/ml at the deepest sample depth of 100 meters.

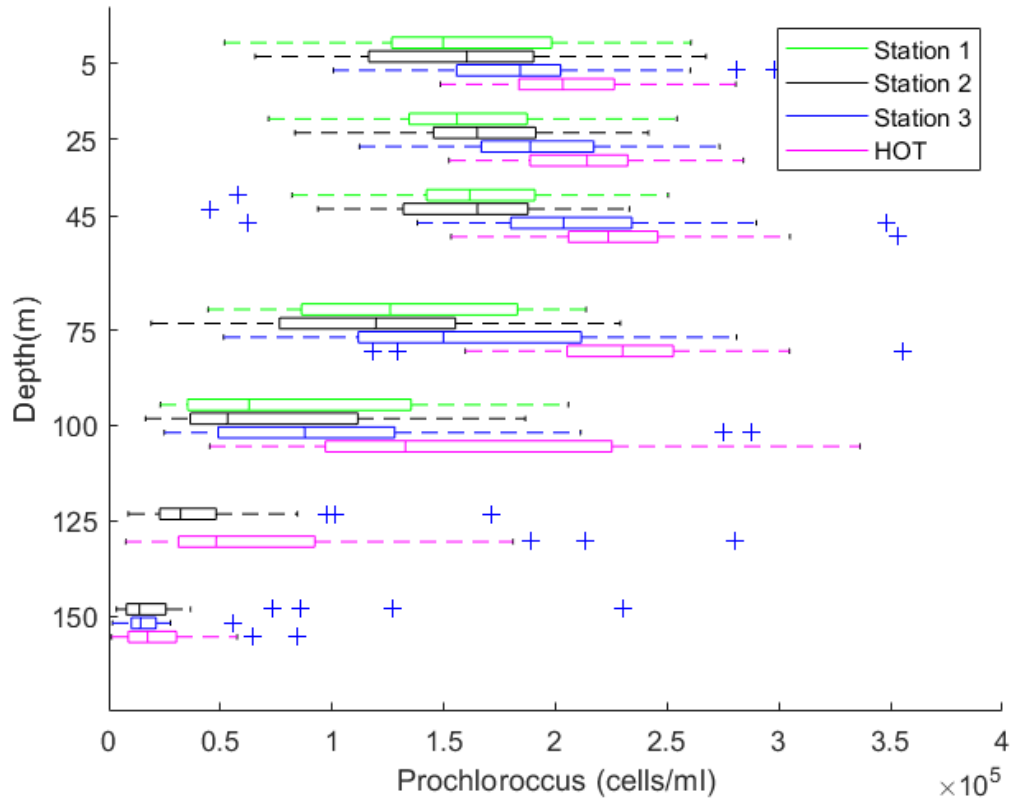


Figure 6. Average cell abundances of *Prochlorococcus* at each sample depth at stations 1, 2, 3, and ALOHA. Boxplots show the 25th, 50th, and 75th percentile and outliers are indicated with plus signs. Samples were collected from Niskin bottles at the depths labeled on the y-axis. Data in green indicates station 1, black is station 2, blue is station 3, and pink is Station ALOHA. Blue plus signs indicate outliers in the data.

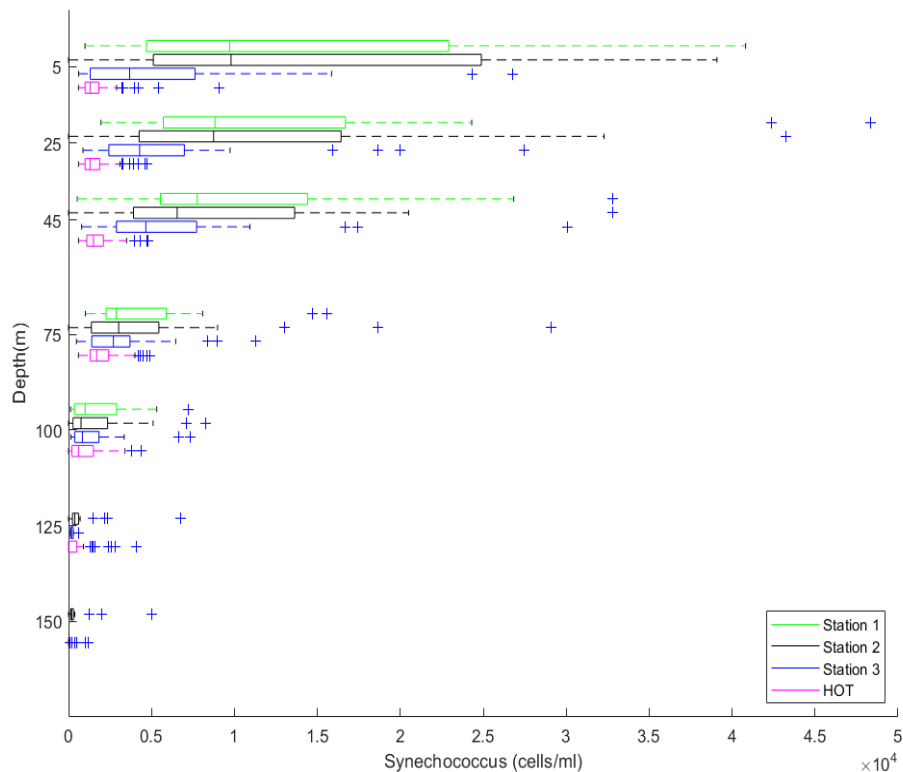


Figure 7. Average cell abundances of *Synechococcus* at each sample depth at stations 1, 2, 3, and ALOHA. Boxplots show the 25th, 50th, and 75th percentile and outliers are indicated with plus signs. Samples were collected from Niskin bottles at the depths labeled on the y-axis. Data in green indicates station 1, black is station 2, blue is station 3, and pink is Station ALOHA. Blue plus signs indicate outliers in the data.

3.3 Comparisons with Oceanographic Measurements

3.3.1 Māhala Bay Comparisons

Chlorophyll-a. There was no linear relationship observed between chlorophyll-a concentrations and *Prochlorococcus* or *Synechococcus* abundance. Figure 8 (A,B,C) shows that maximum *Prochlorococcus* abundances do not align with maximum chlorophyll concentrations. There is no clear relationship between *Synechococcus* cells and chlorophyll concentrations as shown in Figure 8 D,E,F. Where chlorophyll is less than 0.5 $\mu\text{g/l}$, cell counts vary by ten-fold for both populations. A wide variability of cell

counts was observed in comparison to chlorophyll-a concentrations; no clear relationship was observed between chlorophyll concentrations with the *Synechococcus* abundance maximum or the *Prochlorococcus* abundance maximum.

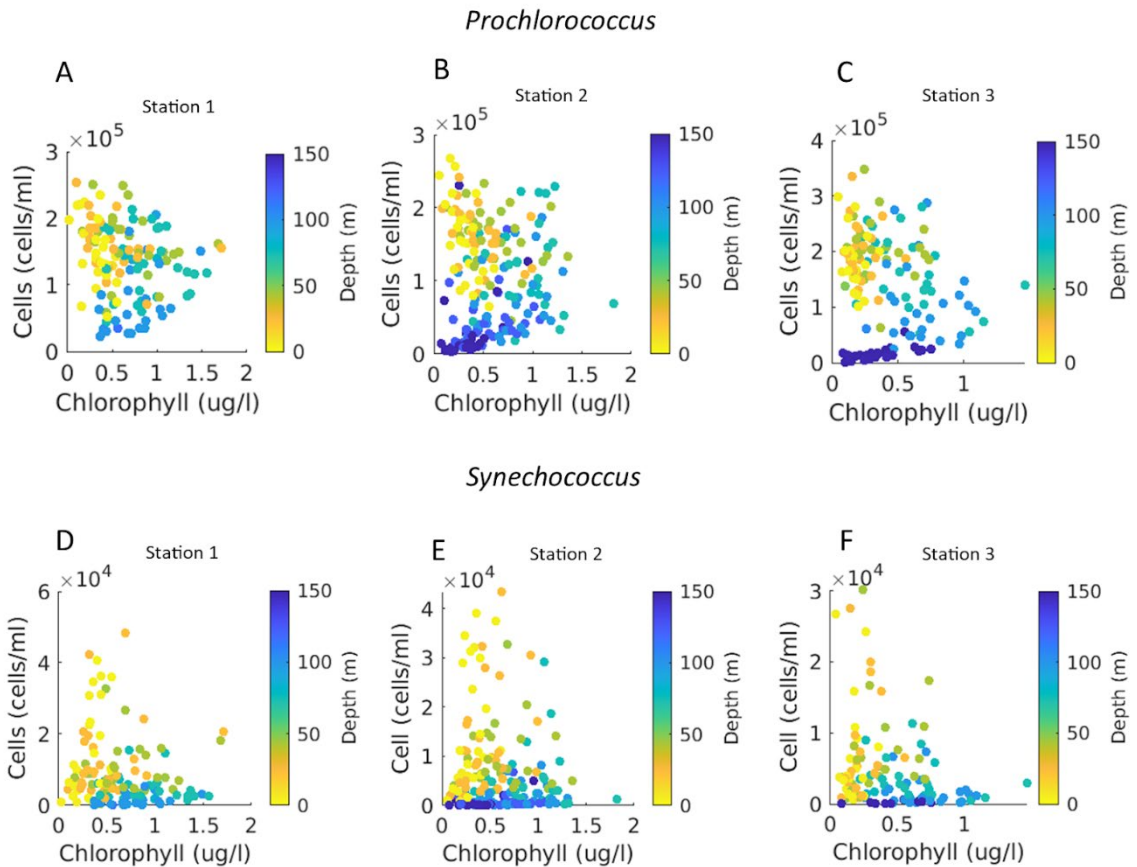


Figure 8. Comparisons between picoplankton cell abundances and chlorophyll concentrations. Lighter colors indicate depths closer to the surface, and darker colors indicate deeper depths towards 150 meters. Measured chlorophyll-a values are plotted against (A) Station 1 of *Prochlorococcus* cell counts (B) Station 2 of *Prochlorococcus* cell counts (C) Station 3 of *Prochlorococcus* cell counts (D) Station 1 of *Synechococcus* cell counts (E) Station 2 of *Synechococcus* cell counts and (F) Station 3 of *Synechococcus* cell counts.

Nutrients. When nutrients and cell counts are plotted on a logarithmic scale, there is a clear inverse relationship. Nutrients are classified as nitrite and nitrate concentrations in $\mu\text{mol/kg}$. The nutrient concentrations increase as cell counts decrease (Figure 8).

Prochlorococcus counts do not reach 10^3 magnitude where nitrate is at its highest concentration (until 150 meters); they stay within the 10^4 magnitude. *Synechococcus* counts do not go lower than 10^2 magnitude where nitrate is at its highest concentration (until 150 meters). *Prochlorococcus* varied within the upper and lower magnitude of 10^5 , and *Synechococcus* varied within the upper and lower magnitude of 10^4 . Station 3 had cell counts of *Synechococcus* in the 10^3 magnitude. The negative trend became more defined at 75 meters and deeper.

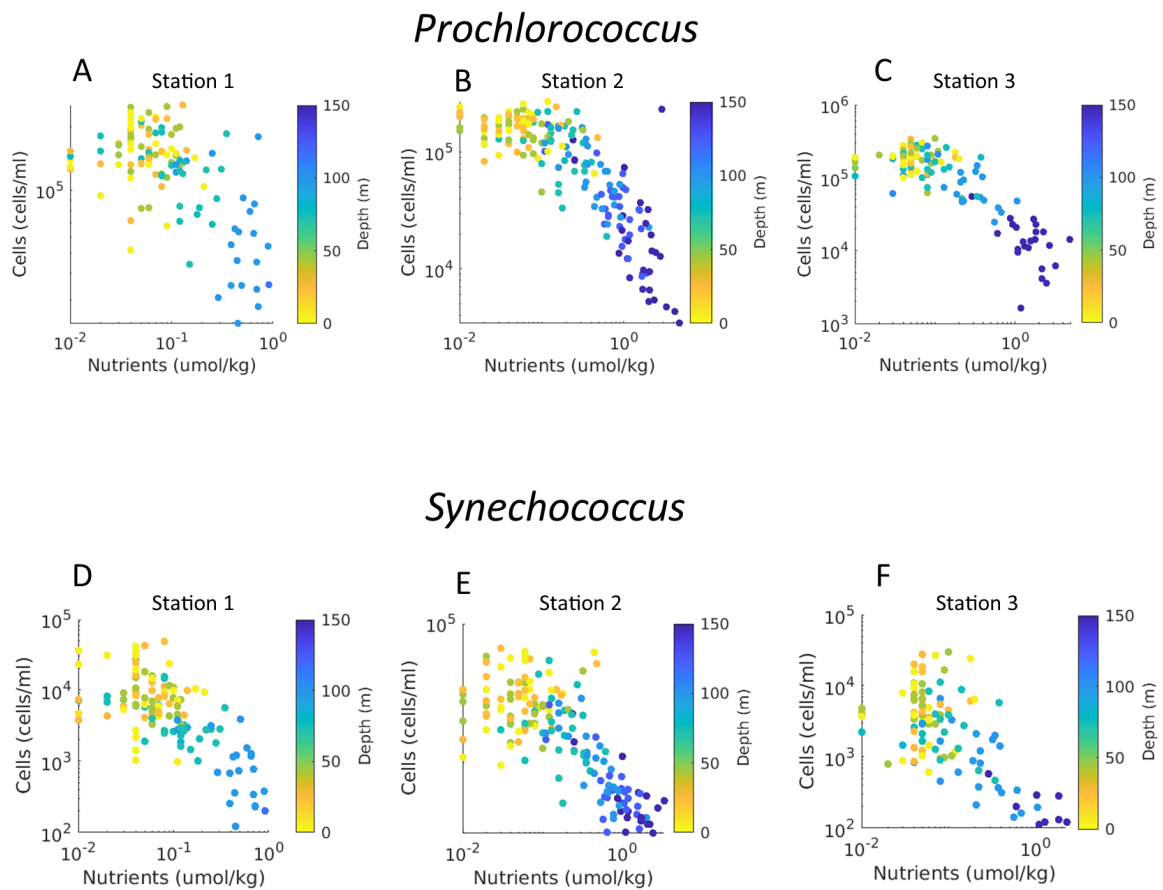


Figure 9. Comparisons between picoplankton cell abundances and nitrate concentrations. Lighter colors indicate depths closer to the surface, and darker colors indicate deeper depths towards 150 meters. Cell counts and nitrate concentrations are shown on a logarithmic scale. Plots show nitrate concentrations versus (A) Station 1 of *Prochlorococcus* cell counts (B) Station 2 of *Prochlorococcus* cell counts (C) Station 3 of *Prochlorococcus* cell counts (D) Station 1 of *Synechococcus* cell counts (E) Station 2 of *Synechococcus* cell counts (F) Station 3 of *Synechococcus* cell counts

PAR. There is a clear positive trend between increasing cell counts and increasing PAR as shown in Figure 10. When plotted on a logarithmic scale, their relationship is linear (Figure 10). Cell counts are highest where PAR is highest, and cell counts are lowest where PAR is lowest. We can divide these trends into three distinct sections of upper (0-50), middle (50-100), and deep (100-150) euphotic zone. The comparison at station 3 shows that while PAR decreases from the surface to about 50 meters, cell counts remain relatively constant at a 10^5 magnitude. For *Synechococcus* distribution, the upper section does not exceed 10^5 magnitude, the middle section sees a range from 10^3 - 10^4 magnitude, and the deep section has $<10^3$ magnitude.

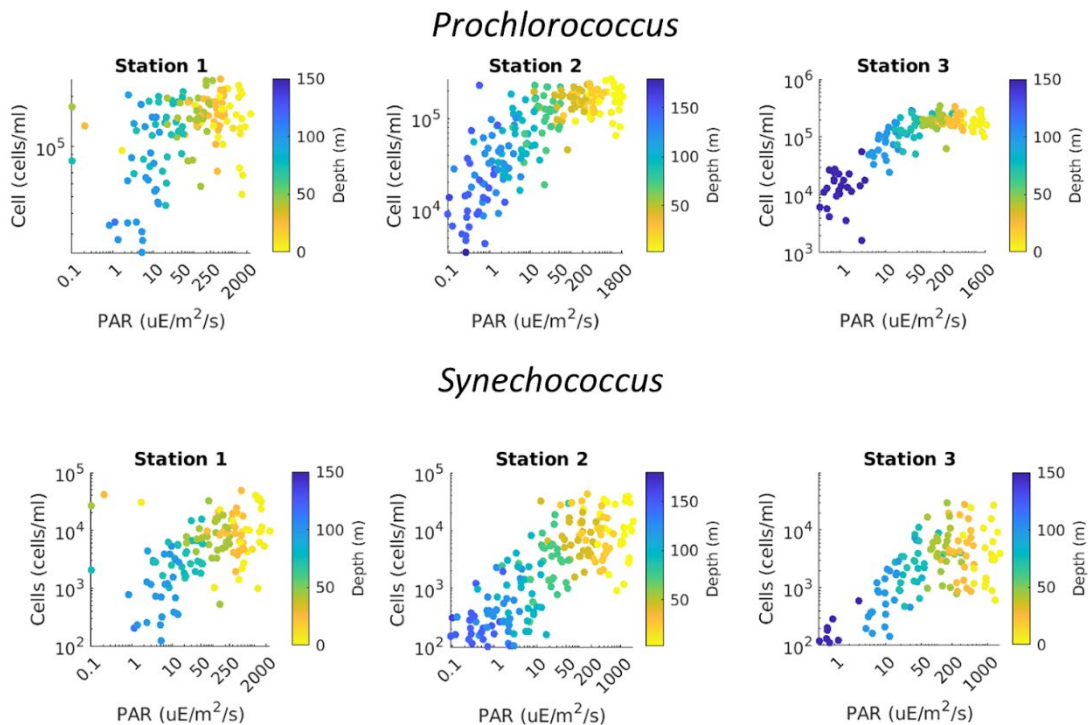


Figure 10. Comparisons between picoplankton cell abundances and PAR at their respective depths. Lighter colors indicate depths closer to the surface, and darker colors indicate deeper depths towards 150 meters. Plots show PAR versus (A) Station 1 of *Prochlorococcus* cell counts (B) Station 2 of *Prochlorococcus* cell counts (C) Station 3

of *Prochlorococcus* cell counts (D) Station 1 of *Synechococcus* cell counts (E) Station 2 of *Synechococcus* cell counts (F) Station 3 of *Synechococcus* cell counts

3.3.2 Station ALOHA Comparisons

Chlorophyll. *Prochlorococcus* and *Synechococcus* display very different relationships with chlorophyll concentrations at Station ALOHA. Figure 11A shows *Prochlorococcus* abundance maximums do not align with the chlorophyll maximums that ranged between 100 and 125 meters. While not a tight relationship, a DCM is distinguishable by the increasing chlorophyll concentrations until this depth before decreasing. There is no clear correlation between *Synechococcus* cell counts and chlorophyll concentrations. There is no clear trend between *Synechococcus* and the overall ecosystem chlorophyll levels; *Synechococcus* counts have a high variance at all chlorophyll concentrations (Figure 11B).

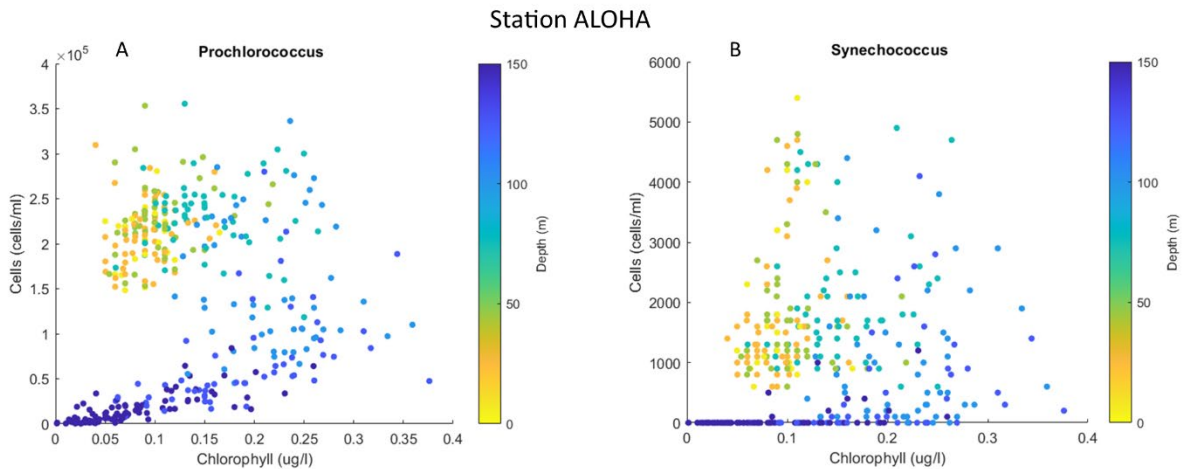


Figure 11. Comparisons between cell abundances and chlorophyll at their respective depths. Lighter colors indicate depths closer to the surface, and darker colors indicate deeper depths towards 150 meters, given the scale of the color bar (right-hand side). (A) shows the correlation between *Prochlorococcus* cells with chlorophyll, and (B) shows the correlations between *Synechococcus* cells with chlorophyll.

Nitrate. The low concentration of nitrate makes it difficult to observe any relationship between cell abundances and nutrients in Figure 12. *Prochlorococcus* counts

remained relatively constant between 25-75 meters depth (Figure 12A), and *Synechococcus* counts were too variable at each sample depth to determine a negative relationship in the first 50 meters. The relationship between *Prochlorococcus* abundances and nitrate concentrations was negative deeper than the mixed layer. *Prochlorococcus* cell counts decreased with depth, while nitrate concentration increased with depth. We begin to see the rapid increase of nitrate between 100 and 125 meters depth- where nitrate reaches approximately 0.1 $\mu\text{mol/kg}$. Cell counts begin a rapid decrease at 100-125 meters as well. There is no clear relationship between *Synechococcus* abundances and nutrient availability in the upper 150 meters at Station ALOHA.

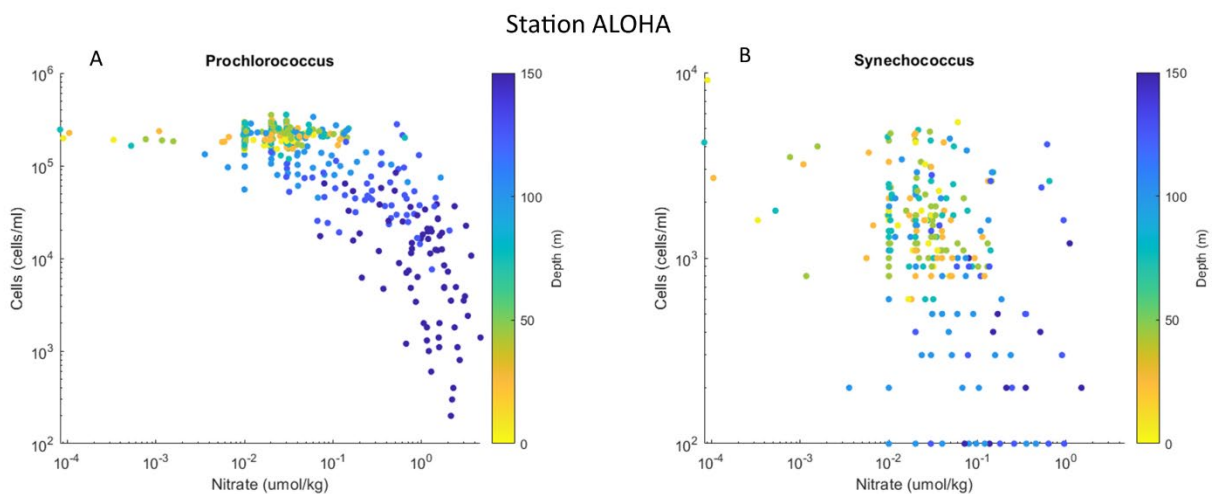


Figure 12. Correlations between cell abundances and nutrients at their respective depths. Lighter colors indicate depths closer to the surface, and darker colors indicate deeper depths towards 150 meters, given the scale of the color bar (right-hand side). (A) shows the correlation between *Prochlorococcus* cells with nutrients, and (B) shows the correlations between *Synechococcus* cells with nutrients.

3.4 Seasonal Variations

By splitting the profiles of each picoplankton population into seasons, we are able to better understand how environmental parameters affect the vertical distribution of *Prochlorococcus* and *Synechococcus*.

Station 1. The MLD at station 1 had a range of 35.1-47.0 meters. Compared to the nutricline and the DCM, the MLD does not shift vertically as much. The shallowest MLD was during the summer (35.1 meters), and the deepest MLD was during the winter (47.0 meters). The DCM and the nutricline reached their deepest depths at 78.0 meters and 71.7 meters in the summer months (Table 2). The DCM was present at a shallower depth than the nutricline in the fall: 47.2 meters compared to 65.8 meters. The upward and downward seasonal shifts of the MLD, DCM, and nutricline corresponded with most of the depths for the subsurface maximums for *Prochlorococcus* and *Synechococcus*, typically in the spring and summer months (Figure 13).

Table 2 Nutricline and DCM depths for station 1 compared to MLD depth. Depths are recorded in meters.

Station 1	Winter	Spring	Summer	Fall
MLD (m)	47.0	38.4	35.1	39.8
Nutricline (m)	71.7	53.3	71.7	65.8
DCM (m)	69.4	71.2	78.0	47.2

Prochlorococcus. The deepest subsurface maximum was located at 45 meters in the summer months, where the MLD was just 10 meters above. Winter and spring months had cell abundance maximums at 25 meters. Figure 13A also shows a drastic decrease in cell abundances between 75 and 100 meters during the spring and summer.

Prochlorococcus cells experienced an increase between 25-45 meters in the fall but did not exceed the abundance at the surface where it was highest.

Synechococcus. For *Synechococcus* cells, no clear subsurface maximum was observed in any season, and there was no clear correlation with the MLD, DCM, or nutricline as shown in Figure 13A. The highest surface cell counts occurred in the spring and summer at almost 2.0E4 cells/ml (Figure 13A). Each season had a decreasing trend from the surface to 100 meters. Cell counts at the bottom of the sample depth existed in 10³ magnitude.

Station 2. The MLD has a wider range at station 2 compared to station 1. The MLD ranged from 37.2-58.7 meters. The DCM reaches its deepest depth in the summer at 85.1 meters and its shallowest in the fall at 49.2 meters (Table 3). The DCM depth becomes shallower than the nutricline depth in the fall. The nutricline depth is deepest in the fall at around 77.5 meters.

Table 3 Nutricline and DCM depths for station 2 compared to MLD depth. Depths are recorded in meters.

Station 2	Winter	Spring	Summer	Fall
MLD (m)	58.7	37.2	40.9	40.5
Nutricline (m)	70.0	66.7	68.0	77.5
DCM (m)	71.3	74.3	85.1	49.2

Prochlorococcus. Subsurface maximums of *Prochlorococcus* cells in the spring and summer are at 45 meters, both corresponding with the MLD. A second decrease in cell counts in the summer occurs at 75 meters, 7 meters below the summer nutricline. The fall months had a subsurface maximum at 25 meters, but this distribution did not seem to correlate with any of the parameters. The *Prochlorococcus* distribution does not correspond with any environmental parameters in the winter.

Synechococcus. *Synechococcus* distribution had an overall decreasing trend with depth. We saw a subsurface maximum in the winter at about 25 meters. The maximum in the summer occurred at 45 meters, but it did not exceed about 2.0E4 cells/ml measured at the surface (top 5 meters). The *Synechococcus* maximum in the summer was the only subsurface maximum that corresponded with the MLD.

Station 3. The mean MLD had a range of 43.2-53.5 meters at station 3. The nutricline did not extend deeper than the DCM depth. The deepest DCM depth occurred in summer at 107.8 meters, and the deepest nutricline depth occurred in spring at 87.5 meters. Each season saw a maximum in abundance with most of them corresponding with the MLD.

Table 4. Nutricline and DCM depths for station 3 compared to MLD depth. Depths are recorded in meters.

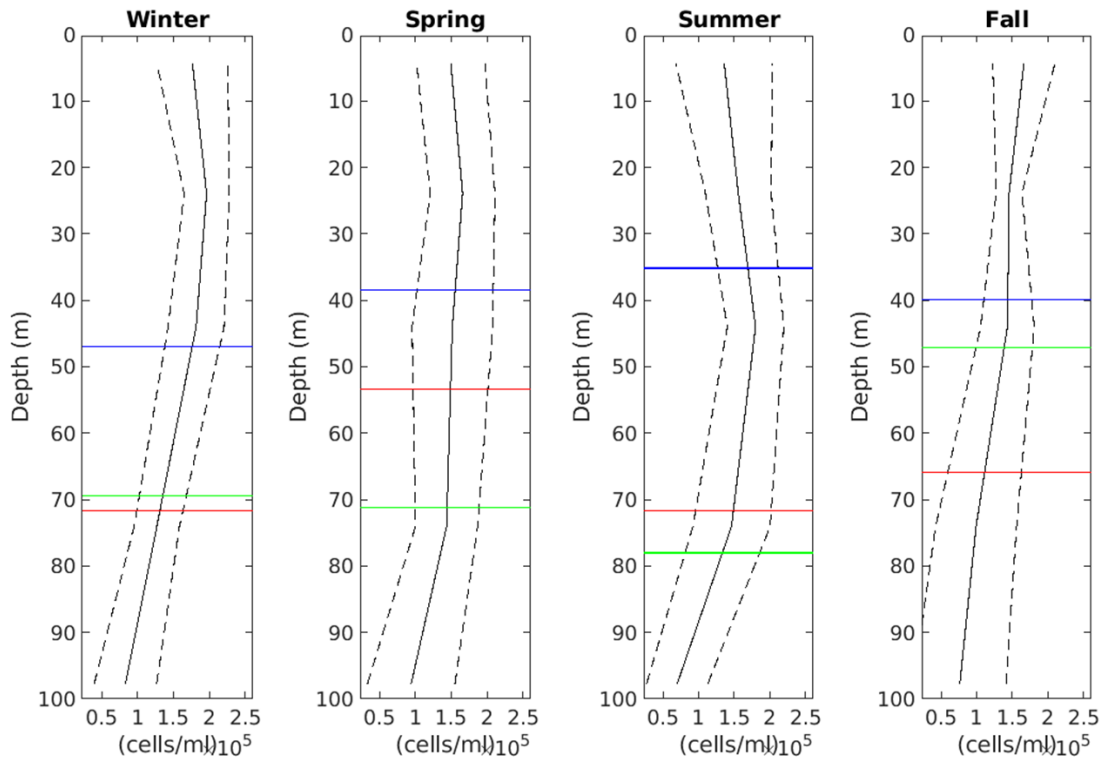
Station 3	Winter	Spring	Summer	Fall
MLD (m)	43.6	43.2	44.0	53.5
Nutricline (m)	77.5	87.5	86.3	66.0
DCM (m)	84.2	96.0	107.8	90.5

Prochlorococcus. *Prochlorococcus* reached cell maximums at 45 meters in the winter and spring, 75 meters in the summer, and a slight maximum in the fall between 25-30 meters. A second point of decrease occurs at 75 meters, 11 meters below the nutricline.

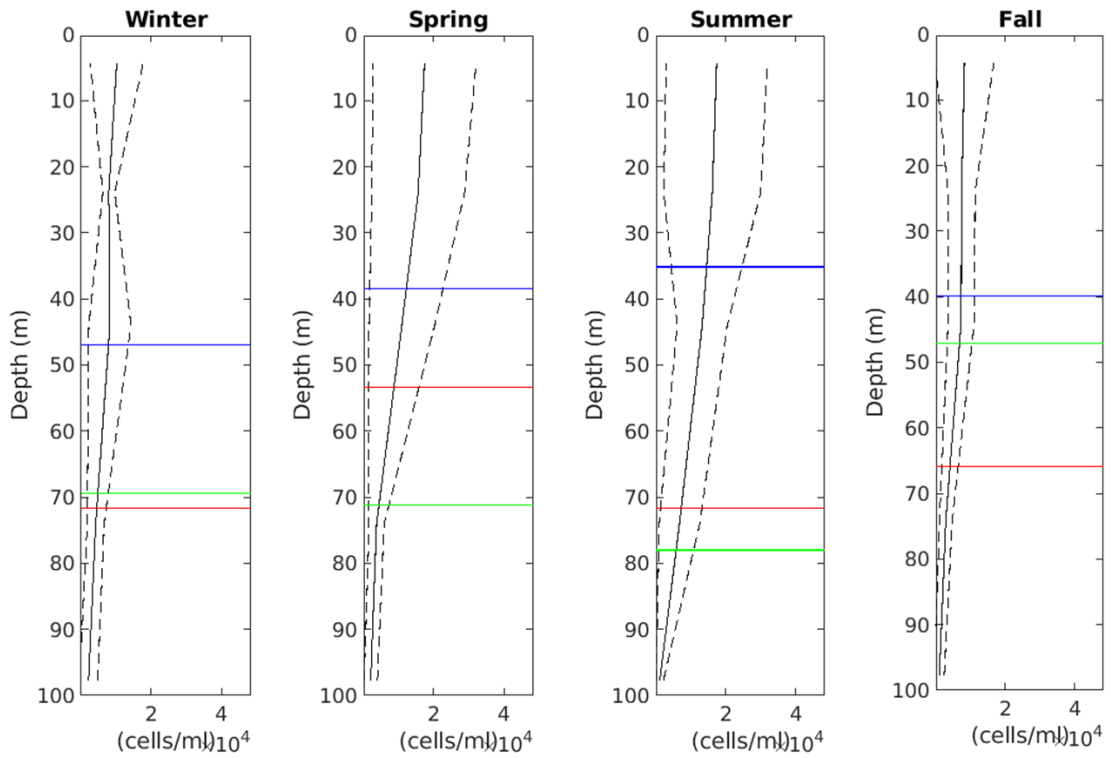
Synechococcus. *Synechococcus* abundances experienced maximums at 45 meters in winter, summer, and fall. The spring maximum occurred at 25 meters. Only the winter and summer maximums correlated with MLD. *Synechococcus* cells decreased before the

DCM or the nutricline could have any influence on the distribution. It is at station 3 that *Synechococcus* abundances have the clearest subsurface maximums.

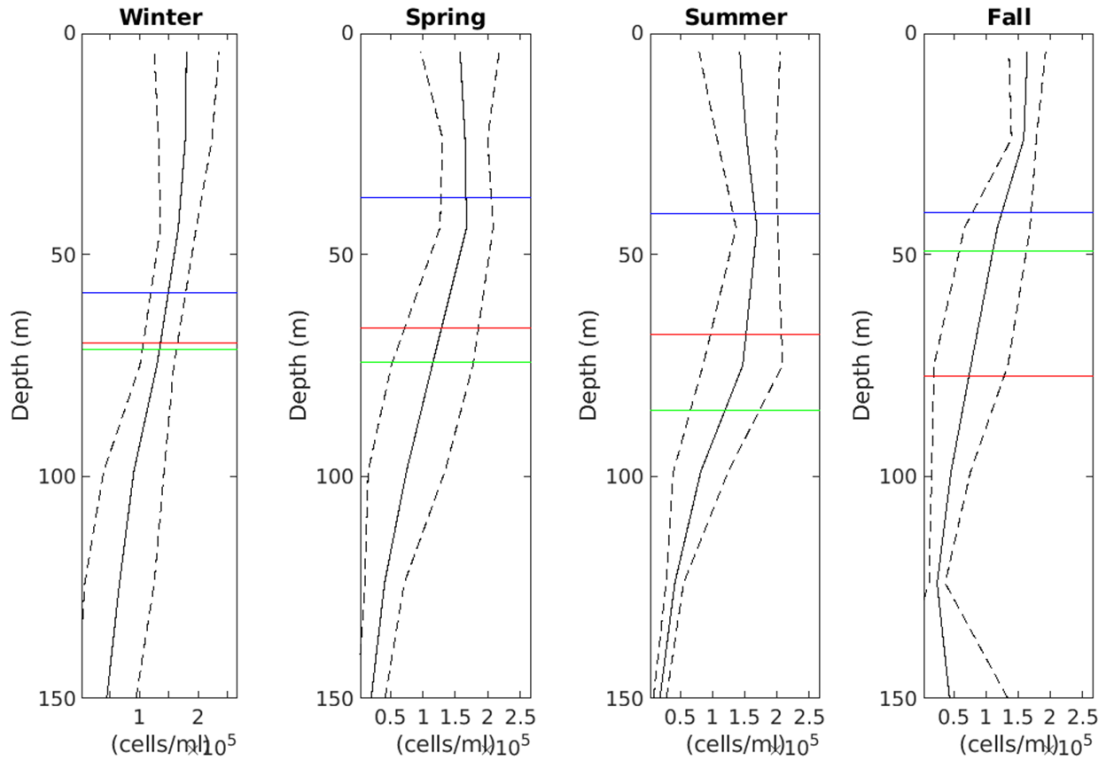
Prochlorococcus



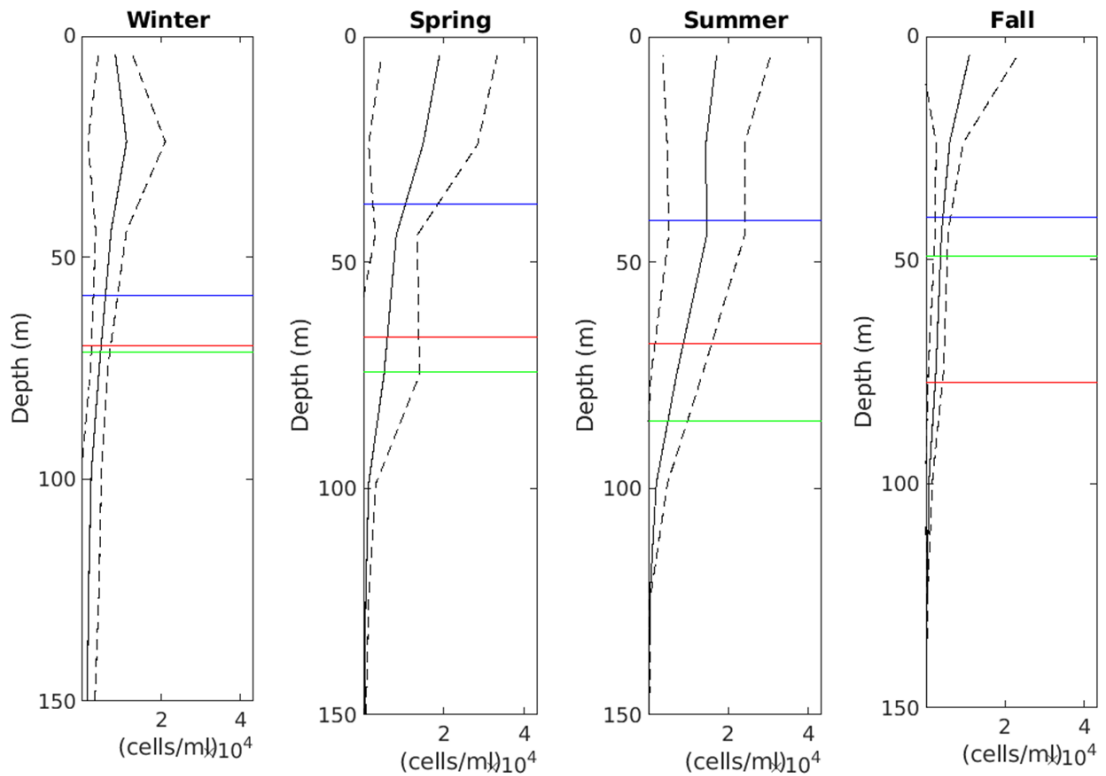
Synechococcus



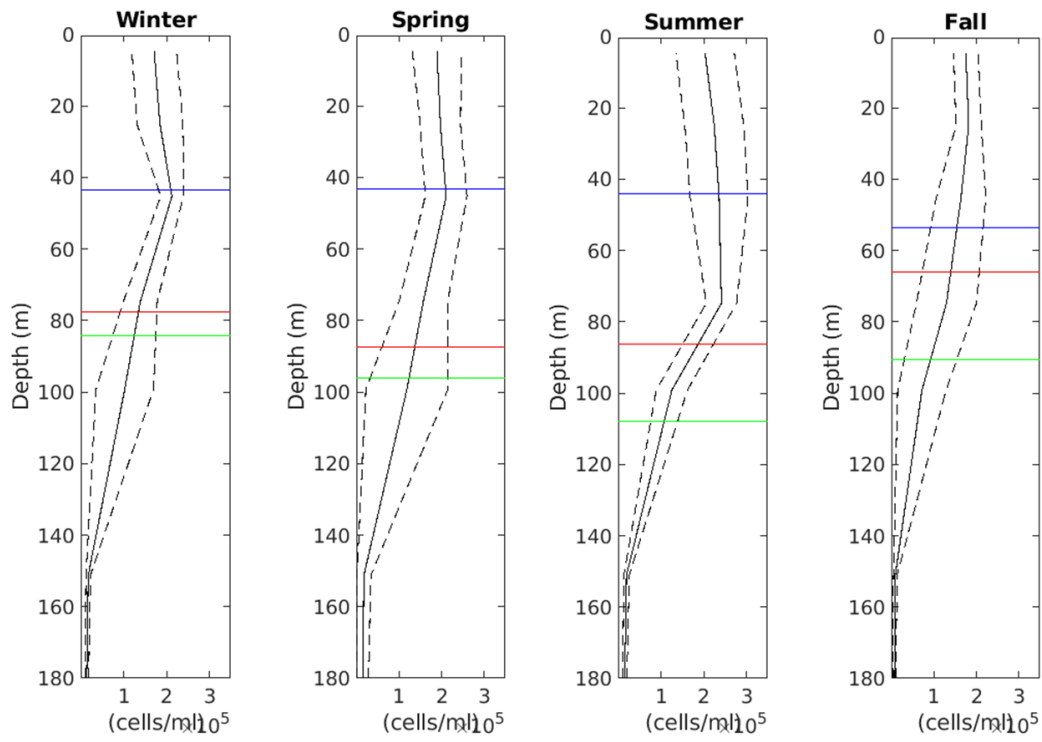
Prochlorococcus



Synechococcus



Prochlorococcus



Synechococcus

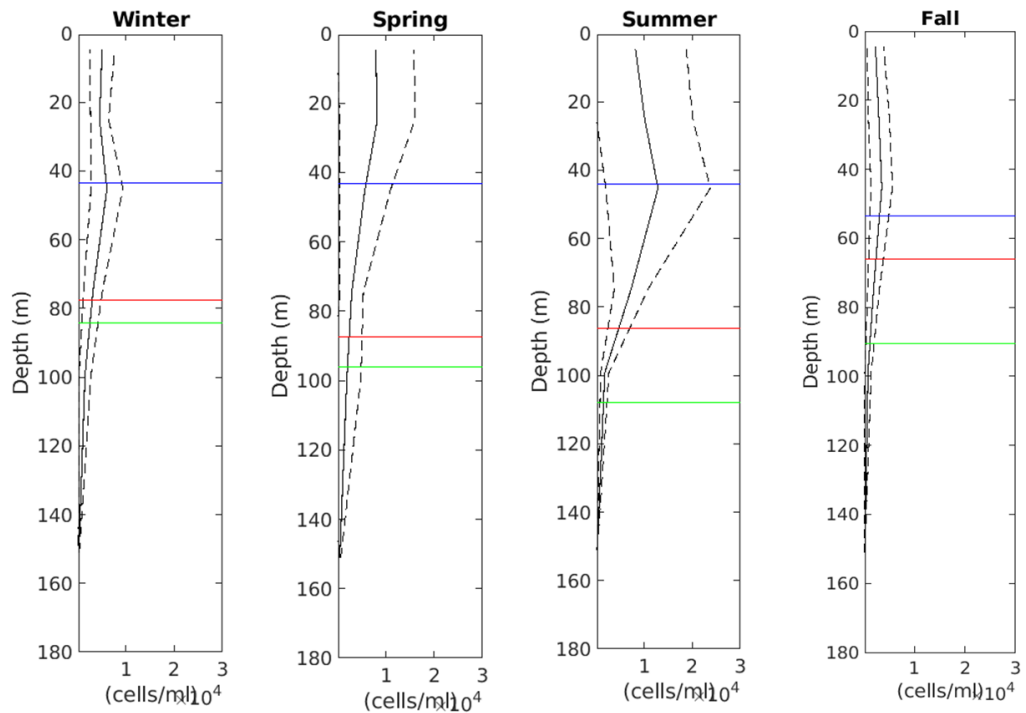


Figure 13. *Prochlorococcus* and *Synechococcus* profiles split into seasons. Profiles include MLD (blue), nutricline (red), and DCM (green) depths separated by station. The

first set of graphs shows the seasonal cell distributions of Station 1, the second set of graphs shows the seasonal cell distributions of Station 2, and the third set of graphs shows the seasonal cell distributions of Station 3.

4.0 DISCUSSION

4.1 Nearshore Distribution of *Prochlorococcus* and *Synechococcus*

Partensky et al. (1999) described *Prochlorococcus* distribution in oligotrophic waters as abundant at the surface mixed layer and decreasing below the thermocline with *Synechococcus* having a parallel distribution of similar magnitude. Partensky's (1999) distribution recognizes a generalization that picoplankton distribution is related to temperature and mixed layer depth. Karl and Letelier (2008) further describe the dependence of phytoplankton primary production on nitrogen fixation in the open ocean. From the results of Māmalā Bay, we can examine the cell abundance from Māmalā Bay in the context of the nutricline and DCM depths. The decreasing concentrations of picoplankton with depth in Māmalā Bay appeared to be strongly related to PAR and nutrients. Cell abundances corresponded positively with PAR and negatively with nutrients. At Station ALOHA, we see a similar correlation between *Prochlorococcus* cells and nutrients in Figure 12A. *Synechococcus* is restricted to depths of higher nutrients in the NPSG, typically at the surface and/or regions of mixing. (Campbell et al. 1997). In this case, Māmalā Bay contained higher concentrations of nitrate compared to Station ALOHA.

There were no direct relationships between cell abundances and DCM depths at either Māmalā Bay or Station ALOHA. This may be because there are other phytoplankton present (not enumerated in this study) determining the depth of the DCM. The contributions of the total chlorophyll from *Prochlorococcus* and *Synechococcus* were not determined from the samples in this study. The pore size of the chlorophyll filters used for chlorophyll-a analysis measured 0.7 μm in size, which can allow more than half

of *Prochlorococcus* and *Synechococcus* to pass through and be unaccounted. This source of error also contributes to unclear chlorophyll-cell count relationships (Figures 8 and 11). In comparing Māmala Bay chlorophyll profiles with Station ALOHA, we can see that the proximity to the island is correlated with chlorophyll-a concentrations, and that the presence of the island plays a role in the environmental influences on vertical picoplankton distribution.

The island of O‘ahu acts as the nutrient supplier for phytoplankton growth. This is evident in the *Synechococcus* distribution in Figure 5. Nitrate concentrations between Māmala Bay and Station ALOHA are similar for the first 25 meters. At around 45 meters, nitrate concentrations at each of the 3 stations in Māmala Bay begin to exceed nitrate concentrations of Station ALOHA. The island mass effect is evident in the increased chlorophyll content at the stations in Māmala Bay (Figure 3). This increase corresponded with the average maximum cell abundance in Figures 6 and 7.

Prochlorococcus and *Synechococcus* abundances in Māmala Bay experienced rapid decreases between 45 and 75 meters. This pattern was detected most strongly at stations 1 and 2, indicating the delayed island mass effect Messie et al. (2020) explained. The island mass effect is seen at all stations when compared to Station ALOHA. There is significantly less chlorophyll at the corresponding depths of Station ALOHA than each of the Māmala Bay stations (Figure 3). Some increases in cell abundances corresponded with the MLD. Below the mixed layer depth, nutrient concentrations may begin to increase, and if there is sufficient PAR, phytoplankton can increase in abundance. This is why some subsurface maxima occurred between the MLD and the 1% light level: this region may have increased nutrients while still enough PAR for phytoplankton growth.

Nitrate is likely depleted at the surface, in part, as a result of *Prochlorococcus* cells existing in the 10^5 magnitude and *Synechococcus* cells existing in the 10^4 magnitude. PAR has the expected relationship of large cell abundances at depths of high PAR values. The decrease in *Prochlorococcus* and *Synechococcus* cell abundances between 45 and 75 meters depth corresponded with environmental parameters. Both nearshore stations had deep chlorophyll maximums at 75 meters depth. The offshore station and Station ALOHA had deeper chlorophyll maximums between 100 and 125 meters depth. Nutrient and PAR influences added to the MLD influence have set the vertical distribution of *Prochlorococcus* and *Synechococcus* in a nearshore environment.

Prochlorococcus and *Synechococcus* maintained the same orders of magnitude between every station with *Prochlorococcus* abundances exceeding *Synechococcus* abundances by one order of magnitude. At Station ALOHA, *Prochlorococcus* distribution had a similar shape, but *Synechococcus* distributions between Station ALOHA and Māhala Bay were almost reversed. *Synechococcus* abundance was greater at stations 1 and 2. Here, we can see the effect of the island mass effect introducing nutrients from the island of O‘ahu.

4.2 Seasonality

The depths of the nutricline, DCM, and MLD shifted seasonally at each station. The MLD had the least movement between seasons and between stations among the three parameters. Profiles that had a second deeper maximum experienced it between the nutricline and DCM depths. These deeper maximums would occur after a region of no notable decreases between depths- typically between 45 and 75 meters. It is at these

deeper maximums that *Prochlorococcus* abundances correspond with the nutricline. This was most common among *Prochlorococcus* distributions, most notably in the summer. Weather events with the greatest impact in southern O‘ahu could be the consistent trade winds in the summer that drive the MLD to deeper depths and may also contribute to the subsurface maxima observed in the *Prochlorococcus* distributions (Figure 13). The fluctuation of the MLD did not seem to have a clear effect on the fluctuation of the nutricline or DCM depth. In the fall months at stations 1 and 2, the DCM would be shallower than the nutricline. The varying depths of the water column at each site may have an influence on the depth of the DCM, meaning that Station 1 typically had the shallowest DCM and nutriclines, and station 3 had the deepest, with station 2 between them. In contrast to Station ALOHA, Māmalā Bay had subsurface maximums of both *Prochlorococcus* and *Synechococcus* in the summer. Station ALOHA only showed subsurface cell maximums in the summer for *Prochlorococcus* (Campbell et al. 1996).

4.3 Ecosystem Services

Ecosystem services are benefits to humans provided by the natural environment and healthy ecosystems (*World Health Organization*). The services provided by a marine ecosystem of Māmalā Bay include carbon removal/sequestration from the atmosphere and providing the base of the food chain for fisheries. The subtropical North Pacific Ocean is described as having homogenous physical and biological properties as seen in studies from the Hawaii Ocean Time Series (Campbell et al. 1997). The environmental factors of nutrients and PAR influenced the vertical picoplankton distribution in a way that is unique to a nearshore ecosystem. The chlorophyll and *Synechococcus*

concentrations in Māmala Bay are enhanced compared to Station ALOHA, and an onshore-offshore gradient was observed where the stations closest to the island had the strongest enhancement chlorophyll and *Synechococcus* concentrations. The island mass effect causes more nutrient-rich conditions in Māmala Bay, allowing *Synechococcus* abundances to exist at much higher magnitudes than at Station ALOHA. The gradient between onshore and offshore picoplankton distributions shows how the introduction of land-based nutrients and near-island upwelling do impact an ecosystem. Understanding how the vertical picoplankton distribution responds to the environmental parameters in the nearshore setting allows us to explore ecosystem services of picoplankton such as carbon fixation and nutrient cycling.

5.0 CONCLUSION

The shape of the vertical picoplankton distribution is a reflection of the environmental properties present at each station at Station ALOHA and in nearshore stations near the southern coast of the island of O‘ahu. We learned that nutrients and PAR had the greatest effect on both populations of the nearshore environment. Rapid assimilation of nutrients by picoplankton are evident in oligotrophic settings. This is supported by the increase of nitrate as cell counts begin to abruptly decrease with depth. Furthermore, seasons played a role in the magnitude of shifts of the nutricline and DCM. The cell responses to these factors show how dynamic the nearshore environment can be throughout the year. The cell distributions of Māmala Bay and Station ALOHA shared some similarities in chlorophyll and nutrient distribution. The *Prochlorococcus* distribution between Māmala Bay and Station ALOHA shared a similar shape, but Station ALOHA had higher cell counts as we saw in Figure 6. We observed higher *Synechococcus* counts in Māmala Bay than at Station ALOHA (Figure 7), and even within Māmala Bay, *Synechococcus* counts increased closer to shore. These observations highlight a clear relationship between nutrients and cell counts was present across all stations.

By understanding the ecology of Māmala Bay, we can further understand the ecosystem services of the bay such as carbon fixation and nutrient cycling. This study highlights the understanding the variability of vertical picoplankton distribution in the pelagic and the ecosystem services Māmala Bay provides.

LITERATURE CITED

- Azevedo Correia de Souza, J.M. and Powell, B., 2017. Different approaches to model the nearshore circulation in the south shore of O'ahu, Hawaii. *Ocean Science*, 13(1), pp.31-46
- Assessment, Millennium Ecosystem. *Ecosystems and human well-being*. Vol. 5. United States of America: Island press, 2005.
- Chavez, F.P., Messié, M. and Pennington, J.T., 2010. Marine primary production in relation to climate variability and change.
- Campbell, L., Liu, H., Nolla, H.A. and Vaultot, D., 1997. Annual variability of phytoplankton and bacteria in the subtropical North Pacific Ocean at Station ALOHA during the 1991–1994 ENSO event. *Deep Sea Research Part I: Oceanographic Research Papers*, 44(2), pp.167-192.
- Comfort, C.M., McManus, M.A., Clark, S.J., Karl, D.M. and Ostrander, C.E., 2015. Environmental properties of coastal waters in Mamala bay, Oahu, Hawaii, at the future site of a seawater air conditioning outfall. *Oceanography*, 28(2), pp.230-239.
- Flombaum, P., Gallegos, J.L., Gordillo, R.A., Rincón, J., Zabala, L.L., Jiao, N., Karl, D.M., Li, W.K., Lomas, M.W., Veneziano, D. and Vera, C.S., 2013. Present and future global distributions of the marine Cyanobacteria *Prochlorococcus* and *Synechococcus*. *Proceedings of the National Academy of Sciences*, 110(24), pp.9824-9829.
- Gove, J.M., McManus, M.A., Neuheimer, A.B., Polovina, J.J., Drazen, J.C., Smith, C.R., Merrifield, M.A., Friedlander, A.M., Ehses, J.S., Young, C.W. and Dillon, A.K., 2016. Near-island biological hotspots in barren ocean basins. *Nature communications*, 7(1), pp.1-8.
- Huisman, J., Thi, N.N.P., Karl, D.M. and Sommeijer, B., 2006. Reduced mixing generates oscillations and chaos in the oceanic deep chlorophyll maximum. *Nature*, 439(7074), pp.322-325.
- Karl, D.M. and Letelier, R.M., 2008. Nitrogen fixation-enhanced carbon sequestration in low nitrate, low chlorophyll seascapes. *Marine Ecology Progress Series*, 364, pp.257-268.
- Kato, H. and Phillips, O.M., 1969. On the penetration of a turbulent layer into stratified fluid. *Journal of Fluid Mechanics*, 37(4), pp.643-655.
- Malmstrom, R.R., Coe, A., Kettler, G.C., Martiny, A.C., Frias-Lopez, J., Zinser, E.R. and Chisholm, S.W., 2010. Temporal dynamics of *Prochlorococcus* ecotypes in the Atlantic and Pacific oceans. *The ISME journal*, 4(10), pp.1252-1264.

Messié, M., Petrenko, A., Doglioli, A.M., Aldebert, C., Martinez, E., Koenig, G., Bonnet, S. and Moutin, T., 2020. The delayed island mass effect: How islands can remotely trigger blooms in the oligotrophic ocean. *Geophysical Research Letters*, 47(2), p.e2019GL085282.

Omand, M.M. and Mahadevan, A., 2015. The shape of the oceanic nitracline. *Biogeosciences*, 12(11), pp.3273-3287.

Partensky, F., Blanchot, J. and Vaultot, D., 1999. Differential distribution and ecology of Prochlorococcus and Synechococcus in oceanic waters: a review. *Bulletin-Institut Oceanographique Monaco-Numero Special-*, pp.457-476.

Partensky, F., Hess, W.R. and Vaultot, D., 1999. Prochlorococcus, a marine photosynthetic prokaryote of global significance. *Microbiology and molecular biology reviews*, 63(1), pp.106-127.

Rii, Y.M., Karl, D.M. and Church, M.J., 2016. Temporal and vertical variability in picophytoplankton primary productivity in the North Pacific Subtropical Gyre. *Marine Ecology Progress Series*, 562, pp.1-18.

van den Engh, G.J., Doggett, J.K., Thompson, A.W., Doblin, M.A., Gimpel, C.N. and Karl, D.M., 2017. Dynamics of prochlorococcus and synechococcus at station ALOHA revealed through flow cytometry and high-resolution vertical sampling. *Frontiers in Marine Science*, 4, p.359.